ACS OMEGA

Open Access

http://pubs.acs.org/journal/acsodf

Article

Xuebijing Injection Attenuates Heat Stroke-Induced Brain Injury through Oxidative Stress Blockage and Parthanatos Modulation via PARP-1/AIF Signaling

Lin Wang,[‖] Boxin Ye,[‖] Yongrui Liu, Jun Li, Chunhe Li, Minyong Wen,* and Hongbo Li*

Cite This: *ACS Omega* 2023, 8, 33392−33402

Read Online

ACCESS | Metrics & More | Article Recommendations

ABSTRACT: Heat stroke (HS) is a potentially fatal acute condition caused by an interplay of complex events including inflammation, endothelial injury, and coagulation abnormalities that make its pharmacological treatment a challenging problem. The traditional Chinese medicine Xuebijing injection (XBJ) has been shown to reduce inflammatory responses and prevent organ injuries in HS-induced mice. However, the underlying mechanism of XBJ in HS-induced brain injury remains unclear. In this study, HS-induced rat models and cell models were established to elucidate the effects and underlying mechanisms of XBJ injection on HS-induced brain injury in vivo and in vitro. The results revealed that XBJ injection improved the survival outcome of HS rats and attenuated HS-induced brain injury in a concentration-dependent manner. Subsequently, the reduction in viability and proliferation of neurons induced by HS were reversed by XBJ treatment, while the HS-induced increased ROS levels and neuron death were also inhibited by XBJ injection. Mechanistically, HS activated PARP-1/AIF signaling in vitro and in vivo, inducing the translocation of AIF from the cytoplasm to the nucleus, leading to PARP-1-dependent cell death of neurons. Additionally, we compared XBJ injection effects in young and old age rats. Results showed that XBJ also provided protective effects in HS-induced brain injury in aging rats; however, the treatment efficacy of XBJ injection at the same concentration was more significant in the young age rats. In conclusion, XBJ injection attenuates HS-induced brain injury by inhibiting oxidative stress and Parthanatos via the PARP-1/AIF signaling, which might provide a novel therapeutic strategy for HS treatment.

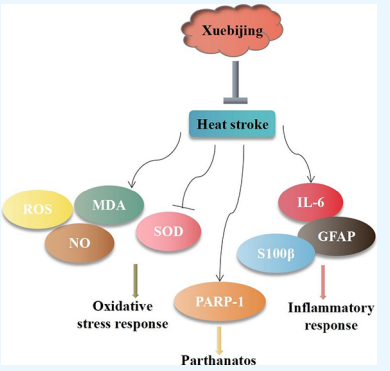

INTRODUCTION

Heat stroke (HS) is a fatal heat-associated disease that results from exposure to a hot environment or strenuous exercise and is reported with an increased incidence rate in recent years due to global warming and widespread heat waves.[1,2] This disease is characterized by a core body temperature over 40.5 °C and is associated with a generalized inflammatory response that results in multiple organ dysfunction or failure, with central nervous system (CNS) disorders such as seizures, delusion, and loss of consciousness predominating.[3,4] HS is often accompanied by multiorgan dysfunction and life-threatening risks.[5] Systemic inflammatory response syndromes (SIRS) and CNS collapse are implicated in this disorder,[6] and the elders are particularly vulnerable to HS with 82−92% of increased mortality due to weakened thermoregulatory function and health conditions or complications with other diseases.[7] In particular, the management and treatment of heat-stroke-induced brain injury are still limited due to the inadequate understanding of the pathological mechanisms of HS. Therefore, it is important to shed light on the molecular mechanisms involved in brain injury induced by HS, which will provide a novel insight into the pharmacological treatment of brain injury.

Previous studies have revealed that HS induces oxidative stress and increases the accumulation of reactive oxygen species (ROS), lipid peroxidation, and DNA damage, leading to subsequent cell death.[8] ROS is reported to induce Parthanatos, a novel type of programmed cell death in response to excessive activation of poly (ADP-ribose) (PAR) polymerase-1 (PARP-1). PARP-1 is one of the DNA damage response PARPs for its critical role in DNA damage repair and cell survival.[9,10] Emerging evidence has also demonstrated that Parthanatos is implicated in multiple neurological diseases such as stroke, brain trauma, and Parkinson's disease.[11−14]

Xuebijing (XBJ) injection is an intravenous Chinese herbal therapeutic derived from Radix Paeoniae Rubra (Chishao), Radix Angelica Sinensis (Danggui), Rhizoma Chuanxiong (Chuanxiong), Flos Carthami (Honghua), and Radix Salviae Miltiorrhizae (Danshen).[15,16] It is widely used to inhibit

Received: May 4, 2023
Accepted: July 19, 2023
Published: September 6, 2023

https://doi.org/10.1021/acsomega.3c03084
ACS Omega 2023, 8, 33392−33402

hyperactive inflammation, prevent oxidative stress, neutralize endotoxins, improve microcirculation, and is applied in the treatment of various inflammatory diseases such as sepsis, lung infections, and liver injury.[17−19] Moreover, XBJ injection is demonstrated to attenuate organ injury and inflammation response in the HS mouse model.[20] XBJ injection is also demonstrated to reduce the oxidative stress and inflammatory cytokine levels in HS-induced lung injury, leading to the improved survival of HS rats.[21] XBJ plays a protective role in the treatment of HS by decreasing ROS levels and improving microcirculation functions.[22−25] However, the effect and underlying mechanisms of XBJ in HS-induced brain injury are rarely investigated.

In the present study, we aimed to investigate the function and explicit mechanism of XBJ injection in HS-induced brain injury in young and old rats. HS-induced rat models and cell models were established to elucidate the effects and underlying mechanisms of XBJ injection both in vivo and in vitro. We hypothesized that XBJ alleviates HS-induced brain injury by reducing the ROS levels and inhibiting the activation of the PARP-1-dependent cell death. The findings of our study will underscore the potential of XBJ injection for the therapy of HS-induced brain injury.

MATERIALS AND METHODS

Animals and Treatments. All procedures of the animal experiments were approved by the Institutional Animal Care and Use Committee of The First Affiliated Hospital of Guangzhou University of Chinese Medicine. Adult male Sprague−Dawley rats (SD, Grade SPF, young group: n = 104, 10 weeks old; aging group: n = 104, ≥ 20 months) were provided by the Vital River (Beijing, China) and kept at a constant temperature (24 ± 1 °C) and 12/12-h light/dark cycle with free access to food and water. Rats in the young group and aging group were randomly divided into a normothermic group (Sham), a vehicle-treated HS group (HS), a low dose XBJ-treated HS group (HS + XBJ low), and a high dose XBJ-treated HS group (HS + XBJ high) (26 rats per group). The animals in the Sham and HS groups received a dose of vehicle (1 mL of phosphate-buffered saline/kg of body weight) daily for 3 days. Contrarily, rats in the HS + XBJ low group were intravenously injected with XBJ (Tianjin Chase Sun Pharmaceutical Co., Ltd., Tianjin, China) at a concentration of 4 mg/mL or 10 mg/mL in the HS + XBJ high group daily for 3 days before the experiment. Heat stroke was induced by placing the rats in an artificial climate chamber without food and water at 43 °C, 60 ± 5% humidity for 70 min. The establishment of a successful HS model was considered when mean arterial pressure significantly reduced from the peak to 25 mmHg with a rectal temperature of > 42 °C.[26] Six rats from each group were sacrificed 6 h after heat stroke induction using an overdose of pentobarbital (200 mg/kg) to assess biochemical and inflammation markers as well as histological and ultra-microstructural changes. The remaining rats were used for survival assessment. To determine the time-course of serum IL-6, S100β, and glial fibrillary acidic protein (GFAP) concentrations after heatstroke induction, animals were sacrificed at 0, 2, 6, and 12 h after heatstroke induction.

Histological Examination. Rat brain (hippocampus) tissues in each group were sectioned, fixed in 10% formalin, embedded in paraffin, and sectioned into 4 μm slices. Then, the sections were subjected to hematoxylin (2 g/L) for 5 min and eosin (1%) staining (Beyotime, Shanghai, China) for 3 min or Nissl's staining solution (C0117, Beyotime) for 5 min, followed by observation and imaging under a Nikon Eclipse E800 microscope. According to the results of hematoxylin and eosin staining, the degree of cell shrinkage and nucleus condensation, the integrity of cell membrane, and cell swelling were observed to assess the brain histopathology score. The score was composed of a 0−12 score range. Each classification was further divided into 0 as normal, 1 as mild, 2 points as moderate, 3 points as severe, and 4 points as extremely severe.

Assessing Brain Water Content. The brain edema was determined by measuring brain water content as described briefly.[27] Briefly, the brain of anesthetized animals was removed and placed in pre-weighed glass vials and then weighed (wet weight). The vials were put into an incubator (Memmert, Germany) at 100 °C for 48 h, and then, the brains were weighed again (dry weight). The water content was calculated using a formula: (Wet weight of brain − Dry weight of brain)/Wet weight of brain.

Transmission Electron Microscopy (TEM). Rat brain (hippocampus) tissues were fixed with 2.5% glutaraldehyde (Sigma-Aldrich, Shanghai, China) for 1 h. The tissues were dehydrated and then embedded in epon (Sigma-Aldrich); microtome was applied for the ultra-thin section which was then put on the copper electron microscopy grids, followed by staining with 5% uranyl acetate for 5 min and Reynold's lead citrate for 2 min. Finally, a TEM (Hitachi H7500 TEM, Tokyo, Japan) instrument was applied to photograph the micrographs.

Cell Culture and Treatment. Rat hippocampal neuronal cells were provided by the Procell Life Science & Technology Co., Ltd. (#CP-R107, Wuhan, China). Cells were incubated in RPMI 1640 medium containing 5% FBS and 1/100 penicillin/streptomycin in a humidified incubator with 5% CO_2 at 37 °C. To mimic HS environment in vitro, cells were moved into an incubator with fresh medium and the bottom of the culture dish was put in a circulating water bath at 42 ± 0.5 °C with 5% CO_2 for 3 h, followed by incubation in a normal environment with 5% CO_2 at 37 °C. For the XBJ injection administration, cells were pretreated with XBJ injection for 24 h at 10, 25, or 50 mg/mL concentrations.

Cell Viability. The viability of neuronal cells after indicated treatments was assessed using Cell Counting Kit-8 (CCK-8) assay following the manufacturer's protocols (Dojindo, Japan). Cells were grown in 96-well plates (5×10^3 cells per well) and cultured for 0, 12, 24, and 48 h. Then, 10 μL CCK-8 solution was supplemented and cocultured for another 4 h. Finally, the viability of cells was determined with a microplate analyzer (NanoDrop, USA) at 450 nm.

5-Ethynyl-2′-deoxyuridine (EdU) Assay. The proliferation potential of neuronal cells was measured using an ethynyldeoxyuridine (EdU) detection kit (RiboBio, Guangzhou, China). Neurons after indicated treatments were plated into 24-well plates (0.5×10^6 cells per well). Then, the EdU labeling media (50 μM) was added into the plates and cultured at 37 °C for 2 h. Then, the cells were treated with 4% paraformaldehyde and 0.5% Triton X-100, stained with Apollo fluorescent dye, and nuclei were stained with DAPI for 30 min at ambient temperature. Finally, the cells were mounted and photographed with a confocal microscope (EVOS M5000, Thermo Fisher).

RT-qPCR. The TRIzol reagent (Sigma-Aldrich) was applied for RNA isolation from rat brain (hippocampus) tissues and neuronal cells. The extracted RNA was reverse-transcribed

https://doi.org/10.1021/acsomega.3c03084
ACS Omega 2023, 8, 33392−33402

using the ProtoScript M-MuLV First Strand cDNA Synthesis Kit (New England Biolabs, MA, US). Then, PCR was performed using SYBR Green qPCR SuperMix (Invitrogen, USA) on the ABI PRISM7500 Sequence Detection System following the manufacturer's protocol. The $2^{-\Delta\Delta Ct}$ method was used for gene expression calculation, and GAPDH served as the internal reference control. The primer sequences are shown in Table 1.

Table 1. Primer Sequences Used in the Study

gene	sequence (5′-3′)
PARP-1 (F)	TGGTGGACATTGTGAAAGG
PARP-1 (R)	AGATCCAATACCTGCTCTCC
GAPDH (F)	AACTCCCATTCTTCCACCT
GAPDH (R)	TTGTCATACCAGGAAATGAGC

Western Blot. A Total Protein Extraction Kit (Beyotime) was used to extract the total protein from rat brain (hippocampus) tissues and neuronal cells according to the manufacturer's instructions, and the protein concentration was assessed by an Enhanced BCA Protein Assay Kit (Beyotime). The protein samples (20 μg) were separated by 10% sodium dodecyl sulfate-polyacrylamide gel electrophoresis (SDS-PAGE) gel and then transferred onto nitrocellulose membranes. Next, 5% BSA (Thermo Fisher) was applied to block the membranes for 60 min. Then, the membranes were cultured with the primary antibodies against IL-6 (ab9324, 1:1000, Abcam), S100β (ab52642, 1:1000, Abcam), GFAP (ab68428, 1:1000, Abcam), PARP-1 (ab191217, 1:1000, Abcam), Cleaved PARP-1 (ab32064, 1:1000, Abcam), AIF (*apoptosis*-inducing factor) (ab32516, 1:1000, Abcam), PAR (ab218106, 1:1000, Abcam), and GAPDH (ab8245, 1:2000, Abcam) as the internal reference. After incubating with the corresponding secondary antibodies (ab6721, 1:2000, Abcam), the protein signal was visualized with enhanced chemiluminescence (Pierce, Rockford, IL, USA) and analyzed with the ImageJ software (version 6.0; National Institutes of Health).

Flow Cytometry. The reactive oxygen species (ROS) levels in rat brain (hippocampus) tissues and cells were assessed with an ROS assay kit (Beyotime). Cells after indicated treatments were harvested, washed, and resuspended in serum-free DMEM. The collected samples and cells were stained with 10 μM dichlorofluorescein diacetate (DCFH-DA, Thermo Fisher) in dark for 30 min. Finally, flow cytometry (FACSCanto II; BD Biosciences, San Jose, CA, USA) was used to determine the fluorescence intensity, and the results were analyzed by FlowJo software.

Biochemical Measurement. The supernatant from rat brain tissues and neuronal cells was collected to determine the level of oxidative-stress-related enzymes such as superoxide dismutase (SOD), malondialdehyde (MDA), and nitric oxide (NO) using commercially available kits (Beyotime Biotech, Shanghai, China) following the manufacturer's instructions.

Immunohistochemical (IHC) Staining. The expression of PARP-1 in rat brain tissues was also measured using IHC staining. Briefly, the paraffin-embedded rat brain tissues were dried, deparaffinized with xylene (Sigma-Aldrich) for 20 min twice, and then soaked in 100, 95, 85, and 80% ethyl alcohol. Then, the sections were washed, incubated with 3% H_2O_2 in methanol for 10 min, and sealed with 5% BSA for 60 min. Next, these sections were cultured with anti-PARP-1 (ab191217, 1:1000, Abcam) at 4 °C overnight, followed by culturing with the secondary antibody (ab6721, 1:1000, Abcam) for 60 min at ambient temperature. Then, the sections were dyed using a DAB immunohistochemistry color development kit (Sangon Biotech, China), and hematoxylin (2 g/L) was applied to stain the nuclei for 4 min according to the manufacturer's instructions and mounted and imaged using a microscope.

Immunofluorescence (IF) Staining. IF staining of rat brain tissues and neuronal cells was performed to explore the nuclear translocation of AIF. Briefly, 4% paraformaldehyde was applied to fix the rat brain paraffin-embedded tissue sections and rat neuronal cells, and 10% normal goat serum was used for blockage. After incubating at 4 °C overnight, the sections were incubated with the primary antibody anti-AIF (ab32516, 1:500, Abcam). Subsequently, the sections were cultured with the corresponding secondary antibody (ab6728, 1:1000, Abcam) for 2 h. Then, 1 μg/mL DAPI (4′, 6-diamidino-2-phenylinedole, Solarbio, Beijing, China) was used for nucleus staining for 3 min, and the images were taken under fluorescence microscopy and analyzed with Image-Pro Plus 6.0 software.

NAD^+ Measurement. Rat neuronal cells were grown in a 10 cm^2 plate at 1×10^7 cells per well. After indicated treatments, cells were harvested and resuspended in 100 μL of NAD^+ extraction buffer (Abcam). After heating the extracts at 60 °C for 5 min, assay buffer (20 μL) was added, followed by vortex and centrifugation at 13,000 rpm for 5 min. The supernatant was collected and supplemented into the working reagent containing assay buffer (Bioassay Systems). Finally, a microplate analyzer was applied to determine the optical density at 565 nm.

Comet Assay. Neuron DNA damage was detected using comet assay as previously described.[28] Briefly, neuronal cells (5×10^5 cells/mL) were grown in a 6-well culture plate for 1 day and treated with sevoflurane for 12 h with or without NAC. Next, cell suspension with 0.5% low-melting agarose (Thermo Fisher) was loaded on 1% agarose-precoated slides, which were then soaked in lysing solution for 90 min at 4 °C without light exposure. After electrophoresing the slides in an electrophoresis tray containing TBE buffer (Thermo Fisher) for 25 min, slides were immersed in an alkaline solution (300 mM NaOH, 1 mM Na2EDTA; pH > 13) for 60 min followed by electrophoresis for 25 min. Then, 0.4 M Tris was used for neutralization and 0.03 mg/mL ethidium bromide (EB, Sigma-Aldrich) was added to treat the cells for 20 min in dark. Then, the slides were rinsed with PBS thrice and observed and imaged using a fluorescence microscope (Olympus IX71, Tokyo, Japan).

Enzyme-Linked Immunosorbent Assay Detection. Serum was obtained from blood (3 mL) by centrifugation at 3500 r/min, 4 °C for 10 min). Serum levels of various inflammatory cytokines at different time points were measured by using commercially available kits (IL-6, S100β, and GFAP, Lianshuo Biological Technology, Shanghai, China) following the manufacturer's protocol.

Statistical Analysis. The results were analyzed by GraphPad Prism 8 software (San Diego, CA, USA) and expressed as the mean ± standard deviation from at least 4 independent replicates. Each biological sample was run in triplicate. Multiple comparisons were performed with a one-way analysis of variance followed by a post hoc test. *$p < 0.05$ indicates statistical significance.

https://doi.org/10.1021/acsomega.3c03084
ACS Omega 2023, 8, 33392−33402

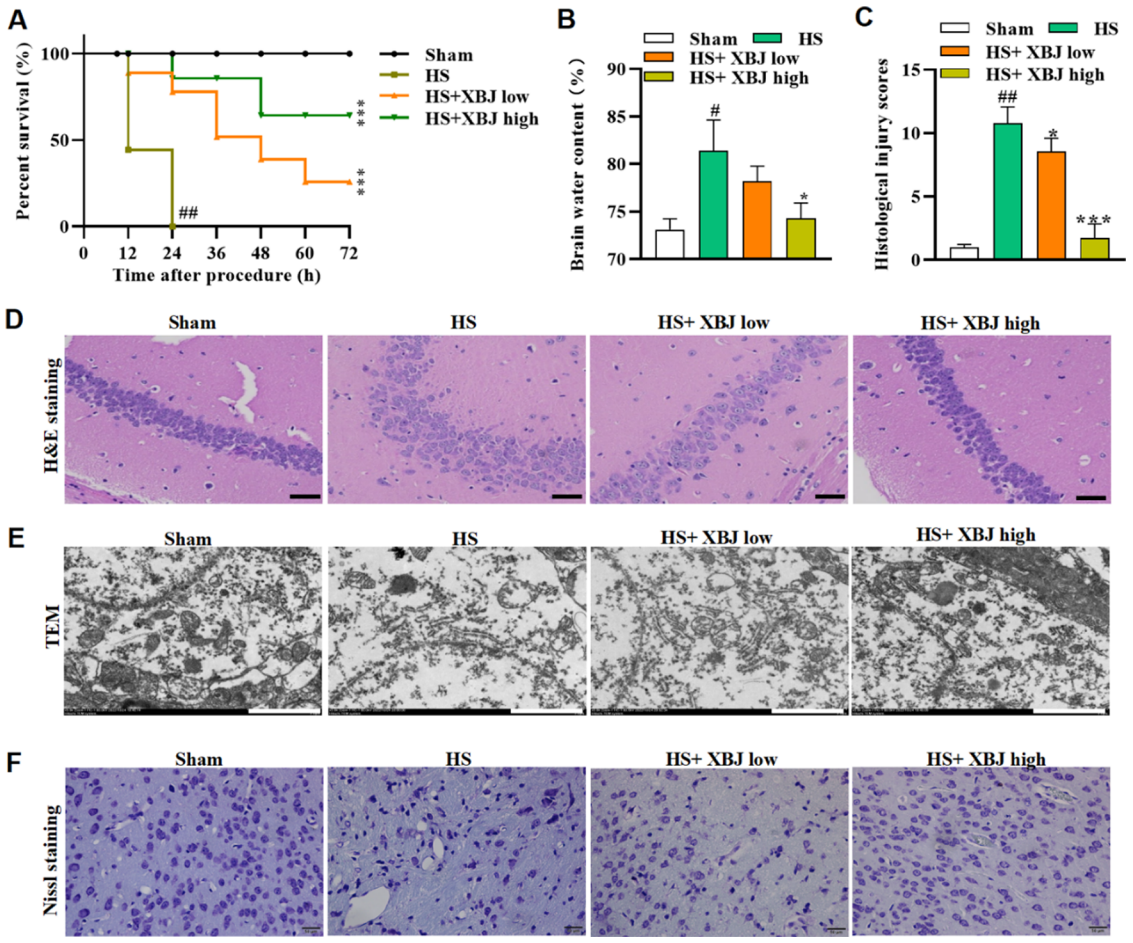

Figure 1. XBJ injection alleviates heat stroke-induced brain injury in vivo. (A) Mean survival time of rats in the sham, HS, HS + XBJ low, and HS + XBJ high groups. (B) Brain water content of rats in indicated groups. (C, D) H&E staining was used to examine the pathological changes of rat brain tissues in indicated groups 6 h after heatstroke induction. Scale bar: 200 μm. (E) Representative TEM images of rat brain tissues in indicated groups 6 h after heatstroke induction. Scale bar: 2 μm. (F) Representative Nissl staining images of the hippocampus tissues of rats. Scale bar: 50 μm. #$p < 0.05$, ##$p < 0.01$ vs Sham group, *$p < 0.05$, ***$p < 0.001$ vs HS group.

RESULTS

XBJ Injection Alleviates Heat Stroke-Induced Brain Injury In Vivo. Heat stroke (HS) rat models were established to probe into the function of XBJ injection on HS-induced brain injury. The mean survival time of rats in the sham, HS, HS + XBJ low (4 mg/mL), and HS + XBJ high (10 mg/mL) groups was measured. We found that the survival time of rats exposed to a high temperature environment was significantly reduced compared with the sham group, while XBJ injection was revealed to improve the survival outcome of HS rats in a dose-dependent fashion (Figure 1A; $p < 0.001$). The brain water content was also measured, and it exhibited a significant increase in the HS group relative to the sham group, while the administration of XBJ injection rescued this increase in a concentration-dependent way (Figure 1B; $p < 0.05$). Furthermore, according to the results of histological staining, rat brain tissues in the sham group showed no pathological changes, and those in the HS group exhibited significant abnormalities with edema, vacant spaces around the neurons and nuclear condensation and loose arrangement of the neurons, which was moderately alleviated by the injection of low concentrations of XBJ, and significantly alleviated in the HS+ XBJ high group (Figure 1C,D; $p < 0.001$). We also observed the morphology of rat brain tissues with a transmission electron microscope (TEM). The HS-induced shrinkage, nucleus condensation, and loss of cell membrane integrity without cell swelling were reversed by XBJ treatment in a dose-dependent way (Figure 1E). Furthermore, we also observed that, after HS injury, the neurons exhibited irregular loosened arrangement and decreased density, and such effects were rescued by XBJ (Figure 1F). Collectively, XBJ injection alleviated heat stroke-induced brain injury in rats.

XBJ Injection Attenuates HS-Induced Neuron Cell Injury In Vitro. The HS in vitro cell models were established by incubating neuron cells in an incubator at 42 ± 0.5 °C with 5% CO_2 for 3 h. To examine the effects of XBJ injection on HS-induced brain cell injury, rat neuronal cells were pretreated with 10, 25, and 50 mg/mL XBJ injection for 24 h. The viability of rat neuronal cells was reduced in the HS group ($p < 0.001$), and the XBJ injection at concentrations of 10 and 25 mg/mL did not significantly affect the viability of rat neurons exposure to hot ambient temperature, while the XBJ at 50 mg/mL significantly rescued the reduction in cell viability induced by HS (Figure 2A; $p < 0.001$). Thus, XBJ at the concentration of 50 mg/mL was applied in the following assays. As revealed by CCK-8 and EdU assays, the proliferation potential of rat neuronal cells was significantly reduced in the HS group ($p < 0.01$ and $p < 0.001$), and XBJ injection was demonstrated to improve the cell proliferation potential compared with the HS

https://doi.org/10.1021/acsomega.3c03084
ACS Omega 2023, 8, 33392−33402

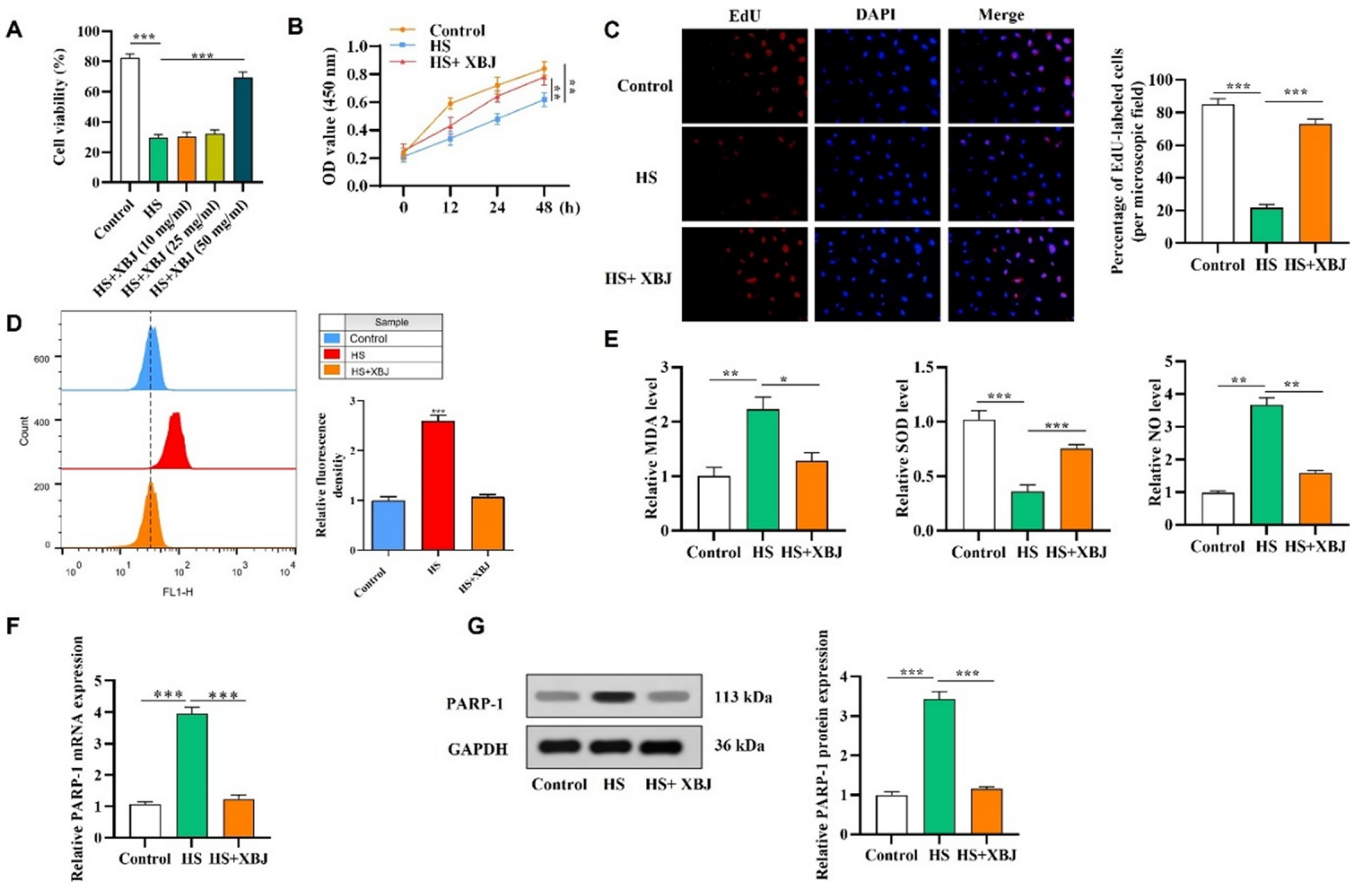

Figure 2. XBJ injection attenuates the HS-induced neuron cell injury. (A) Viability of rat neuronal cells was measured by CCK-8 assays at indicated time points. For XBJ injection treatment, neurons were pretreated with 10, 25, and 50 mg/mL XBJ injection for 24 h before inducing heat stroke. (B, C) Proliferation of rat neuronal cells in the control, HS, HS + XBJ (50 mg/mL) groups was measured using CCK-8 and EdU assays. Scale bar: 100 μm. (D) ROS measurement in neuronal cells in the indicated groups. (E) Levels of MDA, SOD, and NO in rat neuronal cells under indicated treatments. (F, G) RT-qPCR and western blot assays were performed to assess the PARP-1 mRNA and protein levels in rat neuronal cells in indicated groups. *$p < 0.05$, **$p < 0.01$, ***$p < 0.001$.

group (Figure 2B,C; $p < 0.01$ and $p < 0.001$). Furthermore, HS is reported to induce oxidative stress and elevate ROS levels.[8] We therefore next investigated whether XBJ injection could affect the oxidative stress levels of HS-induced cells. We found that HS induced a significant increase in ROS levels in rat neuronal cells ($p < 0.001$), which was revealed to be decreased with the treatment of XBJ injection (Figure 2D; $p < 0.001$). The levels of ROS indicators such as MDA, SOD, and nitric oxide (NO) in rat neurons were detected, and XBJ injection was demonstrated to partially offset the HS-induced elevation in the MDA and NO levels, while upregulated SOD levels in rat neurons (Figure 2E; $p < 0.05$, $p < 0.01$ and $p < 0.001$). Neuron cell death occurs during pathology, and our previous work has revealed that the death rate of neuron cells after HS is approximately 25−30%, which indicates other potential mechanisms of cell death besides apoptosis and autophagy.[29−31] ROS is reported to induce PARP-1-dependent cell death, also named Parthanatos, which is potentially involved in HS-induced brain injury.[32,33] We, therefore, detected the involvement of PARP-1 in HS-induced neuron cells. Our results demonstrated that HS induced an increase in PARP-1 mRNA and protein levels, which was counteracted by the treatment of XBJ injection, suggesting that XBJ injection mitigates the HS-induced Parthanatos of neurons by inhibiting the activation of PARP-1 (Figure 2F,G; $p < 0.001$). Collectively, XBJ injection alleviated heat-stroke-induced Parthanatos of neurons in rats.

XBJ Injection Mitigates ROS Levels and Inflammation Response Induced by HS In Vivo. The effects of HS on ROS and neuroinflammation levels were explored in vivo. We found that HS induced a significant elevation in ROS levels, an upregulation in the levels of MDA, and NO, as well as a downregulation in the level of SOD (Figure 3A,B; $p < 0.01$ and $p < 0.001$). Accordingly, the protein levels of inflammation and brain injury markers such as IL-6, S100β, and GFAP were also found to be significantly increased in the rat brain tissues of the HS group (Figure 3C; $p < 0.01$ and $p < 0.001$), which indicated that HS induces oxidative stress and inflammation response to aggravate the brain injury. Notably, the XBJ injection treatment was revealed to reduce the HS-induced increase in ROS levels, inflammation factor expression, and brain injury maker levels in a concentration-dependent manner (Figure 3A−C; $p < 0.05$, $p < 0.01$, and $p < 0.001$). Collectively, XBJ injection alleviated heat stroke-induced oxidative stress and inflammation response in rats.

XBJ Injection Inhibits Neuron Parthanatos via the PARP-1/AIF Cell Signaling In Vitro. Parthanatos is a type of cell death involved in neuropathological diseases, which is accompanied with PARP-1 overactivation by various stimuli, including DNA damage as well as ROS production.[13] Since we have demonstrated that HS-induced a necrotic morphology

https://doi.org/10.1021/acsomega.3c03084
ACS Omega 2023, 8, 33392−33402

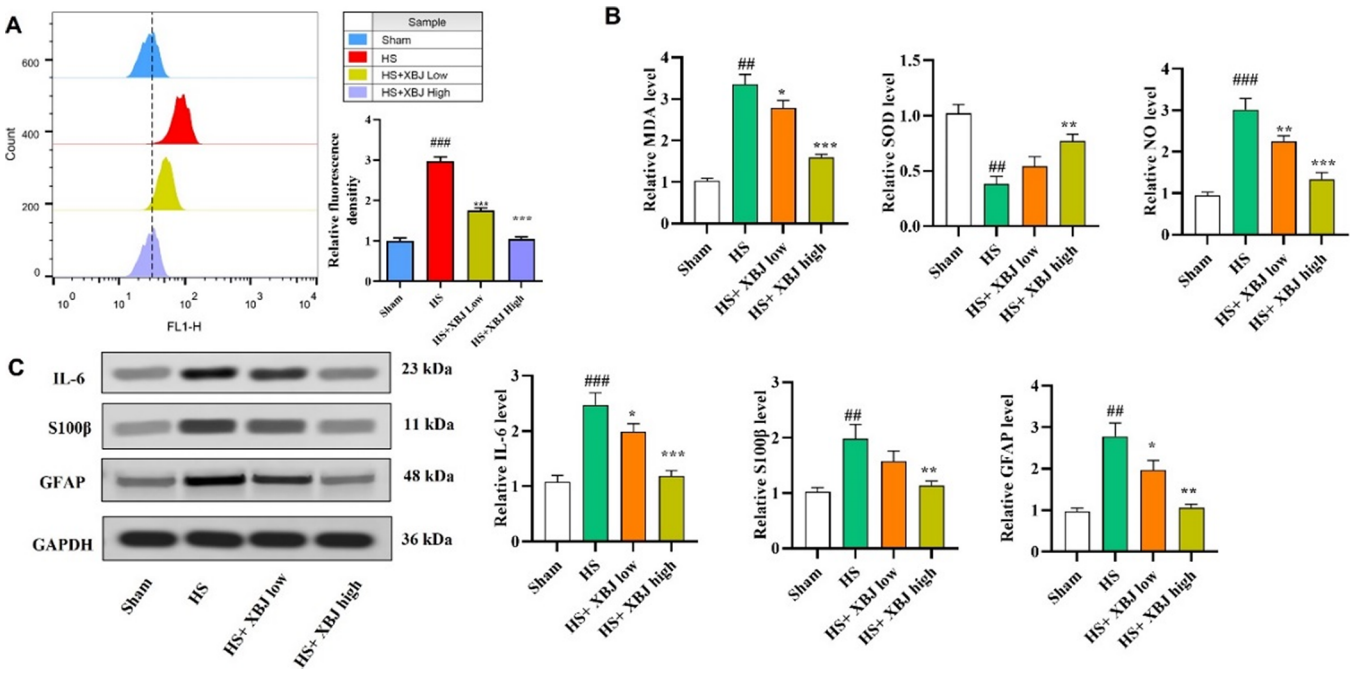

Figure 3. XBJ injection mitigates the ROS levels and inflammation response induced by HS in vivo. (A) Flow cytometry was used to measure the ROS levels in rat brain tissues in indicated groups. (B) Expression of ROS markers in rat brain tissues in different groups. (C) Protein levels of IL-6, S100β, and GFAP in rat brain tissues in the indicated groups. All these parameters were measured at 6 h after heatstroke induction. ##p < 0.01, ###p < 0.001 vs Sham group, *p < 0.05, **p < 0.01, ***p < 0.001 vs HS group.

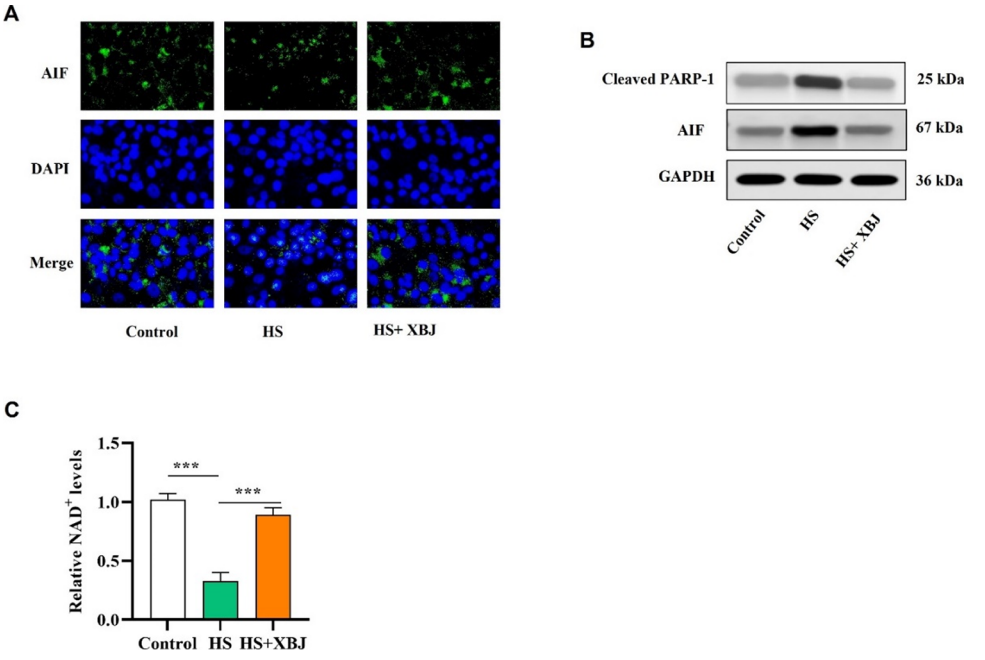

Figure 4. XBJ injection downregulates neuron Parthanatos by inhibiting the activation of the PARP-1/AIF signaling in vitro. (A) Immunofluorescence assays were conducted to explore the AIF nuclear translocation. Scale bar: 50 μm. (B) Protein levels of cleaved PARP-1 and AIF in neurons after the indicated treatment. (C) Cellular content of NAD^+ in neuron cells in the indicated groups. ***p < 0.001.

and promoted the cell death of neurons, we further explored whether HS triggered this type of cell death in vitro. According to the results of immunofluorescence assays, HS promoted the AIF translocation from cytoplasm to the nucleus, which was demonstrated to be suppressed with XBJ injection treatment (Figure 4A). The results of western blot analysis revealed that the protein levels of cleaved PARP-1 and AIF were significantly elevated in the HS group, which was reversed with XBJ injection treatment (Figure 4B). Moreover, the cellular content of NAD^+ in neuron cells was demonstrated to be decreased after HS, however; treatment with XBJ significantly elevated NAD^+ levels in neuron cells relative to the HS group (Figure 4C; p < 0.001). Collectively, XBJ injection inhibited heat stroke-induced neuron Parthanatos via the PARP-1/AIF signaling pathway in vitro.

https://doi.org/10.1021/acsomega.3c03084
ACS Omega 2023, 8, 33392−33402

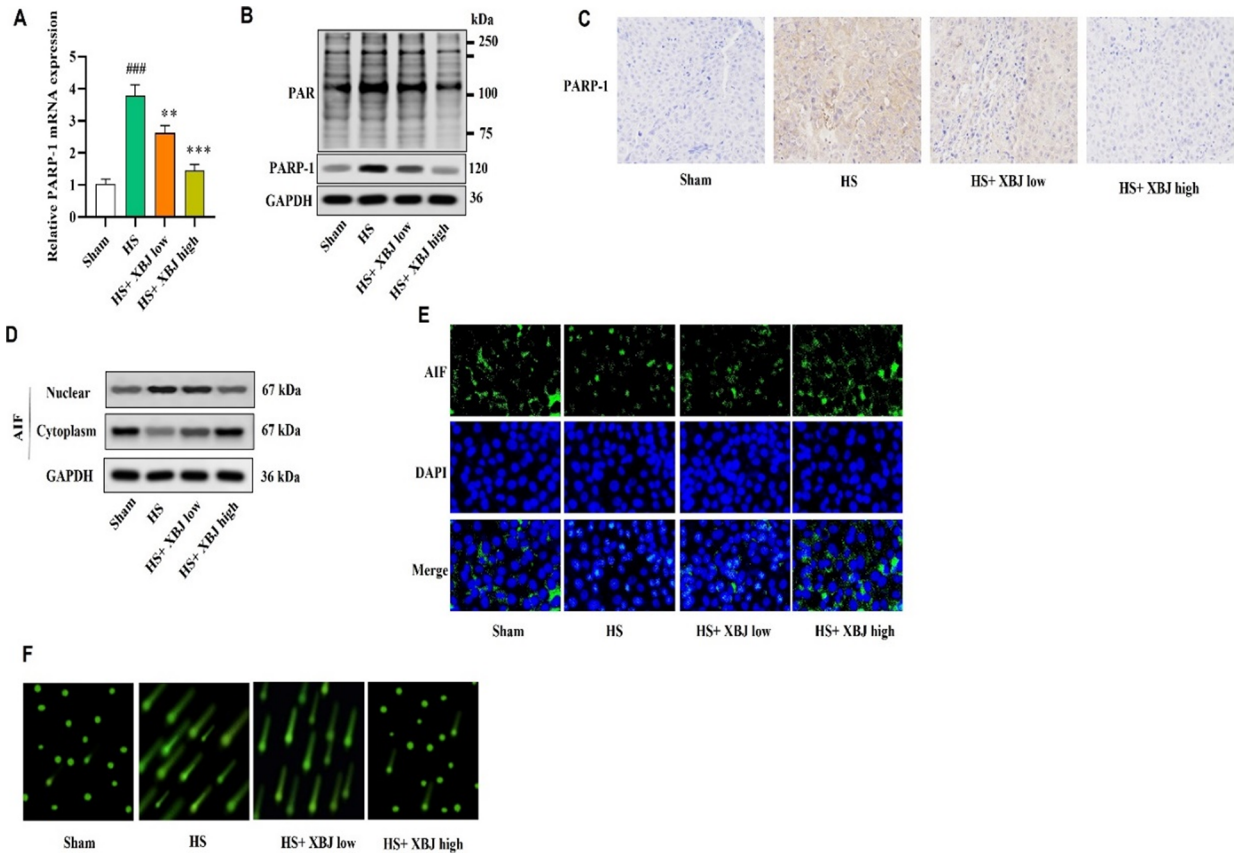

Figure 5. XBJ injection inhibits neuron Parthanatos by suppressing the PARP-1/AIF signaling activation in vivo. (A−C) mRNA and protein levels of PARP-1 in rat brain tissues in indicated groups were measured by RT-qPCR (A), western blot (B), and immunohistochemical staining (C) assays. In addition, PARsylation was shown by western blot (B). Scale bars: 50 μm. (D−E) Translocation of AIF from the cytoplasm to the nucleus was measured using western blot and immunofluorescence staining. Scale bar: 50 μm. (F) DNA damage was measured by comet assays. Scale bar: 50 μm. All these indexes were measured at 6 h after heatstroke induction ###$p < 0.001$ vs Sham group, **$p < 0.01$, ***$p < 0.001$ vs HS group.

XBJ Injection Inhibits Neuron Parthanatos by Suppressing the PARP-1/AIF Cell Signaling Activation In Vivo. We further verified the involvement of Parthanatos signaling in vivo. The levels of PARP-1 in rat brain tissues were measured using RT-qPCR, western blot and immunohistochemical staining, and we found that HS-induced significant elevation of PARP-1 expression in brain tissues ($p < 0.001$), which was moderately mitigated by the treatment of low concentrations of XBJ injection (4 mg/mL) ($p < 0.01$) and significantly reduced by the administration of high concentrations of XBJ injection (10 mg/mL) ($p < 0.001$) (Figure 5A−C). Besides, we also found that PARylation of PARP1 was increased after HS induction, which then decreased by XBJ injection in a dose-dependent way (Figure 5B). The translocation of AIF from the cytoplasm to the nucleus was also increased in the HS group, and XBJ injection was revealed to inhibit the AIF nuclear translocation in a concentration-dependent manner (Figure 5D). Similarly, immunofluorescence staining suggested that HS induced the AIF translocation to the nucleus, which was moderately inhibited by the administration of low concentration of XBJ injection and significantly reduced by high concentrations of XBJ injection treatment (Figure 5E). Moreover, the DNA damage was also measured using comet assays. The results indicated that XBJ injection alleviated the HS-induced DNA damage in a concentration-dependent manner (Figure 5F). Taken together, XBJ injection inhibited heat stroke-induced neuron Parthanatos via the PARP-1/AIF signaling pathway in vivo.

Protective Effects of XBJ in Aging Rats with Heat Stroke. Age is one of the main risk factors for HS, and patients over 60 years of age are faced with 82−92% of excess mortality risks.[7,34] We therefore next explored the effects of XBJ injection on the HS-induced brain injury in elder rats. As shown in Figure 6A, the overall survival rates of the rats in the aging groups were significantly lower than those in the young group ($p < 0.01$). Moreover, the effect of XBJ injection in attenuating HS-induced survival showed better efficacy in the young group relative to the aging group ($p < 0.01$). As expected, H&E staining revealed that XBJ injection in elder rats attenuated the HS-induced edema, vacant spaces around the neurons, nuclear condensation, and loose arrangement of the neurons in hippocampus (Figure 6B; $p < 0.01$ and $p < 0.001$). These results were further confirmed by TEM images, which revealed that the HS-induced shrinkage, nucleus condensation, and loss of cell membrane integrity were reversed by XBJ (Figure 6C). Furthermore, we measured the levels of inflammation and brain injury markers such as IL-6, S100β, and GFAP in the serum of aging rats. We found that the content of IL-6, S100β, and GFAP was elevated in the HS group ($p < 0.001$), and XBJ injection was demonstrated to reduce the levels of these factors in a dose-dependent way ($p < 0.05$ and $p < 0.01$) (Figure 6D). Collectively, XBJ injection inhibited heat stroke-induced heart injury in aging rats.

https://doi.org/10.1021/acsomega.3c03084
ACS Omega 2023, 8, 33392−33402

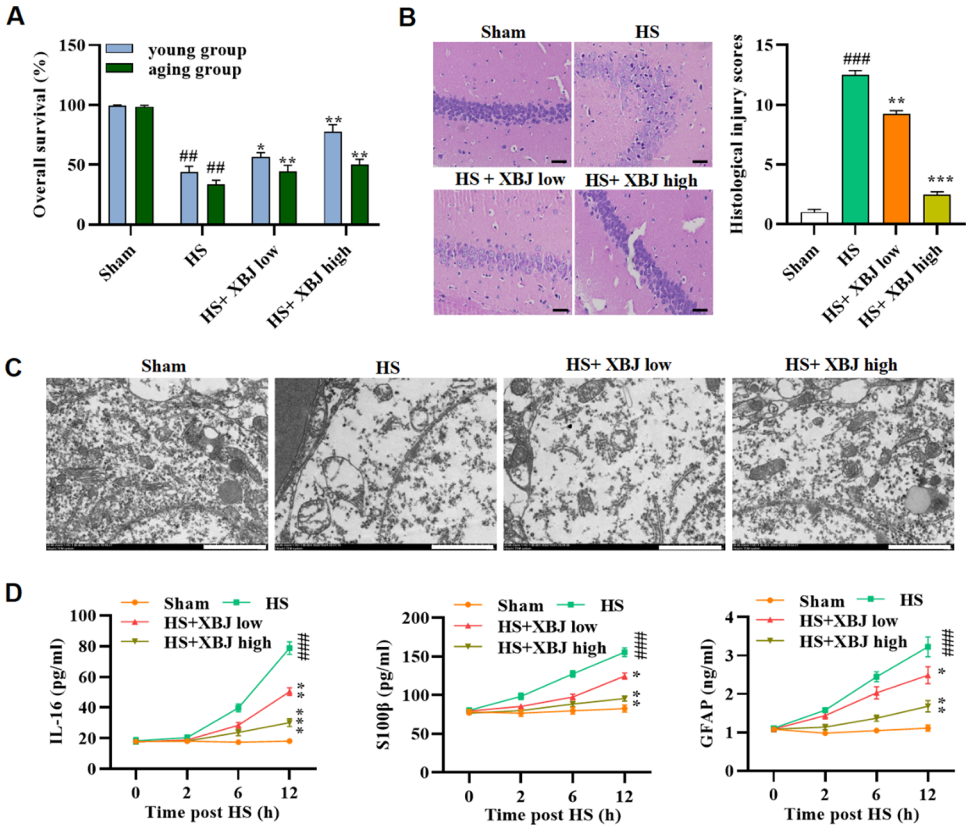

Figure 6. Protective effects of XBJ in aging rats with heat stroke. (A) Overall survival rate of the rats in the aging and young groups after indicated treatments. (B, C) HE staining and TEM were used to explore the effect of XBJ injection on the HS-induced brain injury in aging rats 12 h after heatstroke induction. (B) Scale bar: 200 μm. (C) Scale bar: 500 nm. (D) Levels of inflammation and brain injury markers such as IL-6, S100β and GFAP in the serum of aging rats at indicated time points. ##p < 0.01, ###p < 0.001 vs Sham group, *p < 0.05, **p < 0.01, ***p < 0.001 vs HS group.

DISCUSSION

In this study, we found that XBJ injection alleviated the HS-induced brain injury in vivo and in vitro by relieving the oxidative stress and inhibiting Parthanatos via regulating the PARP-1/AIF cell signaling. XBJ injection was demonstrated to exert a neuroprotective effect against HS-induced brain injury in a dose-dependent way and showed improved efficacy in younger rats compared with aging rats.

CNS maintains body temperature during environmental temperature changes and alters body temperature in response to the declined energy homeostasis in the inflammatory conditions.[35,36] All patients have CNS injury during the early stages of HS, and more than 30% of patients progress to long-term CNS dysfunction.[37−39] The hippocampus is particularly vulnerable to HS, which can induce high mortality or irreversible neurological sequelae. Thus, CNS dysfunction is a primary factor during HS.[40] Alleviating brain injury, especially in the hippocampus region, can improve the survival of HS-stimulated rodents.[41−43] Our research revealed that XBJ alleviated the HS-induced injury in hippocampus and improved survival rate in rats.

HS induces CNS dysfunction, and the increased temperature leads to brain morphological changes in HS animal models.[44] The expression of pro-inflammatory factors such as IL-6, TNF-α, and IL-1β is demonstrated to increase in HS, which indicates that HS induces immune response and promotes severe pathology.[45] Increasing evidence also indicates that the neuroinflammation contributes to the brain injury during heat stroke.[46,47] Previously, it has been shown that XBJ injection has anti-inflammatory effects in HS-induced organ injuries including the liver, heart, and kidney injuries.[20] In agreement with previous publications, we also found that XBJ injection improved the survival outcome of rats with HS. The HS-induced pathological changes and injury in rat brain were revealed to be mitigated by the treatment of XBJ injection in a concentration-dependent manner.

HS is indicated to induce the oxidative stress and stimulate ROS production.[8,48] Several lines of evidence have shown that at the onset of HS, the extent of MDA, and nitric oxide (NO) levels are increased while SOD is reduced.[49,50] In line with the results of these studies, in our study, we also found that HS induced a significant increase in oxidative stress and ROS production. Interestingly, XBJ injection inhibited the HS-induced increase in oxidative stress and ROS production. Moreover, inflammatory injury following exposure to a high-temperature environment is a main pathological feature of HS.[51] We found that the treatment of XBJ reduces the levels of inflammation and injury factors in HS cell and rat models, which suggested the neuroprotective effect of XBJ injection to attenuate the inflammation response and brain injury of HS rats.

PARP-1 excessive activation causes depletion of cellular NAD^+ and ATP, PAR polymer accumulation, as well as mitochondria-nucleus translocation of AIF. This PARP-1-dependent cell death is caspase-independent cell death, which is different from autophagy, apoptosis, and necrosis.[52,53]

https://doi.org/10.1021/acsomega.3c03084
ACS Omega 2023, 8, 33392−33402

Increasing evidence has revealed that ROS promotes the DNA damage and PARP-1 excess activation, leading to PARP-1-dependent cell death.[54,55] In our study, we found that the treatment of XBJ injection exerted a suppressive effect on the PARP-1/AIF signaling activation and DNA damage induced by HS in a concentration-dependent way in vitro and in vivo.

Clinically, it has been demonstrated that the elderly patients are more vulnerable to HS and mortality from HS among the elderly is over 50%.[56,57] Thus, in this study, we explored the protective effect of XBJ injection on the treatment of aging rats with HS. The overall survival of aging rats was significantly lower after HS modeling relative to the young rat group. Moreover, XBJ injection was more effective in the treatment of young rats with HS than aging rats. The high concentration of XBJ injection also mitigated the HS-induced brain injury in aging rats. These results underscore the necessity on HS treatment in aging patients with decreased immune function and complication with other diseases in future studies.

CONCLUSIONS

In summary, we found for the first time that XBJ injection could inhibit the oxidative stress and inflammation response and improve neuron cell survival by blocking the PARP-1-dependent cell death to alleviate HS-induced brain injury in vivo and in vitro. The findings of our study may deepen our understanding of the effect and underlying mechanisms of XBJ injection in the treatment of HS-induced brain injury and provide a theoretical basis for clinical trial and a promising sight for HS-induced brain injury treatment.

ASSOCIATED CONTENT

Data Availability Statement

The datasets generated during and/or analyzed during the current study are available from the corresponding author on reasonable request.

AUTHOR INFORMATION

Corresponding Authors

Minyong Wen − *Department of Critical Care Medicine, The First Affiliated Hospital of Guangzhou University of Chinese Medicine, Guangzhou, Guangdong 510405, China*; Phone: +8613535028852; Email: WMY_ICU@126.com

Hongbo Li − *Department of Critical Care Medicine, The First Affiliated Hospital of Guangzhou University of Chinese Medicine, Guangzhou, Guangdong 510405, China*; orcid.org/0000-0001-6096-1741; Phone: +8613430276760; Email: lihongbo91235@gzucm.edu.cn

Authors

Lin Wang − *Department of Emergency, The First Affiliated Hospital of Guangzhou University of Chinese Medicine, Guangzhou, Guangdong 510405, China*

Boxin Ye − *The First Clinical Medical School, Guangzhou University of Chinese Medicine, Guangzhou, Guangdong 510405, China*

Yongrui Liu − *The First Clinical Medical School, Guangzhou University of Chinese Medicine, Guangzhou, Guangdong 510405, China*

Jun Li − *The First Clinical Medical School, Guangzhou University of Chinese Medicine, Guangzhou, Guangdong 510405, China*

Chunhe Li − *Department of Critical Care Medicine, The First Affiliated Hospital of Guangzhou University of Chinese Medicine, Guangzhou, Guangdong 510405, China*

Complete contact information is available at: https://pubs.acs.org/10.1021/acsomega.3c03084

Author Contributions

‖L.W. and B.Y. contributed equally to this work.

Notes

The authors declare no competing financial interest.

ACKNOWLEDGMENTS

This work was supported by the National Natural Science Foundation of China (No. 82104572) and the Guangzhou Science and Technology Project (Nos. 202102080465 and 202201020339).

REFERENCES

(1) Schramm, P. J.; Vaidyanathan, A.; Radhakrishnan, L.; Gates, A.; Hartnett, K.; Breysse, P. Heat-Related Emergency Department Visits During the Northwestern Heat Wave - United States, June 2021. *MMWR Morb. Mortal. Wkly. Rep.* **2021**, *70*, 1020−1021.

(2) Bouchama, A.; Abuyassin, B.; Lehe, C.; Laitano, O.; Jay, O.; O'Connor, F. G.; Leon, L. R. Classic and exertional heatstroke. *Nat. Rev. Dis. Prim.* **2022**, *8*, 8.

(3) Walter, E. J.; Carraretto, M. The neurological and cognitive consequences of hyperthermia. *Crit. Care* **2016**, *20*, 199.

(4) Lawton, E. M.; Pearce, H.; Gabb, G. M. Review article: Environmental heatstroke and long-term clinical neurological outcomes: A literature review of case reports and case series 2000−2016. *Emerg. Med. Australas.* **2019**, *31*, 163−173.

(5) Peiris, A. N.; Jaroudi, S.; Noor, R. Heat Stroke. *Jama* **2017**, *318*, 2503.

(6) Chang, C. Y.; Chen, J. Y.; Chen, S. H.; Cheng, T. J.; Lin, M. T.; Hu, M. L. Therapeutic treatment with ascorbate rescues mice from heat stroke-induced death by attenuating systemic inflammatory response and hypothalamic neuronal damage. *Free Radical Biol. Med.* **2016**, *93*, 84−93.

(7) Kenny, G. P.; Yardley, J.; Brown, C.; Sigal, R. J.; Jay, O. Heat stress in older individuals and patients with common chronic diseases. *CMAJ* **2010**, *182*, 1053−1060.

(8) Zhang, L.; Li, Y.; Xing, D.; Gao, C. Characterization of mitochondrial dynamics and subcellular localization of ROS reveal that HsfA2 alleviates oxidative damage caused by heat stress in Arabidopsis. *J. Exp. Bot.* **2009**, *60*, 2073.

(9) Yu, S. W.; Wang, H.; Poitras, M. F.; Coombs, C.; Bowers, W. J.; Federoff, H. J.; Poirier, G. G.; Dawson, T. M.; Dawson, V. L. Mediation of poly(ADP-ribose) polymerase-1-dependent cell death by apoptosis-inducing factor. *Science* **2002**, *297*, 259−263.

(10) Wang, Y.; An, R.; Umanah, G. K.; Park, H.; Nambiar, K.; Eacker, S. M.; Kim, B. W.; Bao, L.; Harraz, M. M.; Chang, C.; Chen, R.; Wang, J. E.; Kam, T. I.; Jeong, J. S.; Xie, Z.; Neifert, S.; Qian, J.; Andrabi, S. A.; Blackshaw, S.; Zhu, H.; Song, H.; Ming, G. L.; Dawson, V. L.; Dawson, T. M. A nuclease that mediates cell death induced by DNA damage and poly(ADP-ribose) polymerase-1. *Science* **2016**, *354*, No. aad6872.

(11) Martire, S.; Mosca, L.; d'Erme, M. PARP-1 involvement in neurodegeneration: A focus on Alzheimer's and Parkinson's diseases. *Mech. Ageing Dev.* **2015**, *146-148*, 53−64.

(12) Lee, Y.; Karuppagounder, S. S.; Shin, J. H.; Lee, Y. I.; Ko, H. S.; Swing, D.; Jiang, H.; Kang, S. U.; Lee, B. D.; Kang, H. C.; Kim, D.; Tessarollo, L.; Dawson, V. L.; Dawson, T. M. Parthanatos mediates AIMP2-activated age-dependent dopaminergic neuronal loss. *Nat. Neurosci.* **2013**, *16*, 1392−1400.

(13) Conrad, M.; Angeli, J. P.; Vandenabeele, P.; Stockwell, B. R. Regulated necrosis: disease relevance and therapeutic opportunities. *Nat. Rev. Drug Discovery* **2016**, *15*, 348−366.
(14) Kam, T. I.; Mao, X.; Park, H.; Chou, S. C.; Karuppagounder, S. S.; Umanah, G. E.; Yun, S. P.; Brahmachari, S.; Panicker, N.; Chen, R.; Andrabi, S. A.; Qi, C.; Poirier, G. G.; Pletnikova, O.; Troncoso, J. C.; Bekris, L. M.; Leverenz, J. B.; Pantelyat, A.; Ko, H. S.; Rosenthal, L. S.; Dawson, T. M.; Dawson, V. L. Poly(ADP-ribose) drives pathologic α-synuclein neurodegeneration in Parkinson's disease. *Science* **2018**, *362*, No. eaat8407.
(15) Li, S.; Wang, H.; Sun, Q.; Liu, B.; Chang, X. Therapeutic Effect of Xuebijing, a Traditional Chinese Medicine Injection, on Rheumatoid Arthritis. *Evid. Based Complementary Altern. Med.* **2020**, *2020*, No. 2710782.
(16) Wang, P.; Song, Y.; Liu, Z.; Wang, H.; Zheng, W.; Liu, S.; Feng, Z.; Zhai, J.; Yao, C.; Ren, M.; Bai, C. Xuebijing injection in the treatment of severe pneumonia: study protocol for a randomized controlled trial. *Trials* **2016**, *17*, 142.
(17) Jiang, M.; Zhou, M.; Han, Y.; Xing, L.; Zhao, H.; Dong, L.; Bai, G.; Luo, G. Identification of NF-κB Inhibitors in Xuebijing injection for sepsis treatment based on bioactivity-integrated UPLC-Q/TOF. *J. Ethnopharmacol.* **2013**, *147*, 426−433.
(18) Zhou, W.; Lai, X.; Wang, X.; Yao, X.; Wang, W.; Li, S. Network pharmacology to explore the anti-inflammatory mechanism of Xuebijing in the treatment of sepsis. *Phytomedicine* **2021**, *85*, No. 153543.
(19) Liu, M. W.; Liu, R.; Wu, H. Y.; Zhang, W.; Xia, J.; Dong, M. N.; Yu, W.; Wang, Q.; Xie, F. M.; Wang, R.; Huang, Y. Q.; Qian, C. Y. Protective effect of Xuebijing injection on D-galactosamine- and lipopolysaccharide-induced acute liver injury in rats through the regulation of p38 MAPK, MMP-9 and HO-1 expression by increasing TIPE2 expression. *Int. J. Mol. Med.* **2016**, *38*, 1419−1432.
(20) Xu, Q.; Liu, J.; Guo, X.; Tang, Y.; Zhou, G.; Liu, Y.; Huang, Q.; Geng, Y.; Liu, Z.; Su, L. Xuebijing injection reduces organ injuries and improves survival by attenuating inflammatory responses and endothelial injury in heatstroke mice. *BMC Complement. Altern. Med.* **2015**, *15*, 4.
(21) Chen, Y.; Tong, H.; Pan, Z.; Jiang, D.; Zhang, X.; Qiu, J.; Su, L.; Zhang, M. Xuebijing injection attenuates pulmonary injury by reducing oxidative stress and proinflammatory damage in rats with heat stroke. *Exp. Ther. Med.* **2017**, *13*, 3408−3416.
(22) Jin, H.; Chen, Y.; Ding, C.; Lin, Y.; Chen, Y.; Jiang, D.; Su, L. Microcirculatory Disorders and Protective Role of Xuebijing in Severe Heat Stroke. *Sci. Rep.* **2018**, *8*, 4553.
(23) Ji, J.; Zhou, F.; Yue, H.; Song, Q. Protective mechanism of Xuebijing injection against heat stroke in rats. *Exp. Ther. Med.* **2014**, *7*, 2014.
(24) Sheng, C.; Peng, W.; Xia, Z.; Wang, Y. Plasma and cerebrospinal fluid pharmacokinetics of hydroxysafflor yellow A in patients with traumatic brain injury after intravenous administration of Xuebijing using LC-MS/MS method. *Xenobiotica* **2020**, *50*, 545−551.
(25) Hu, H. X.; Zhu, M. Q.; Sun, Y. C.; Ma, C.; Wang, X.; Liu, X. L. Xuebijing enhances neuroprotective effects of ulinastatin on transient cerebral ischemia via Nrf2-are signal pathways in the hippocampus. *J. Biol. Regul. Homeost. Agents* **2018**, *32*, 1143−1149.
(26) Lin, X.; Lin, C. H.; Liu, R.; Li, C.; Jiao, S.; Yi, X.; Walker, M. J.; Xu, X. M.; Zhao, T.; Huang, P. C.; Sun, G. Myricetin against myocardial injury in rat heat stroke model. *Biomed. Pharmacother.* **2020**, *127*, No. 110194.
(27) Song, J.; Li, N.; Xia, Y.; Gao, Z.; Zou, S. F.; Kong, L.; Yao, Y. J.; Jiao, Y. N.; Yan, Y. H.; Li, S. H.; Tao, Z. Y.; Lian, G.; Yang, J. X.; Kang, T. G. Arctigenin Treatment Protects against Brain Damage through an Anti-Inflammatory and Anti-Apoptotic Mechanism after Needle Insertion. *Front. Pharmacol.* **2016**, *7*, 182.
(28) Piao, M.; Wang, Y.; Liu, N.; Wang, X.; Chen, R.; Qin, J.; Ge, P.; Feng, C. Sevoflurane Exposure Induces Neuronal Cell Parthanatos Initiated by DNA Damage in the Developing Brain via an Increase of Intracellular Reactive Oxygen Species. *Front. Cell. Neurosci.* **2020**, *14*, No. 583782.
(29) Li, H.; Liu, Y.; Gu, Z.; Li, L.; Liu, Y.; Wang, L.; Su, L. p38 MAPK-MK2 pathway regulates the heat-stress-induced accumulation of reactive oxygen species that mediates apoptotic cell death in glial cells. *Oncol. Lett.* **2018**, *15*, 775−782.
(30) Li, H.; Liu, Y.; Wen, M.; Zhao, F.; Zhao, Z.; Liu, Y.; Lin, X.; Wang, L. Hydroxysafflor yellow A (HSYA) alleviates apoptosis and autophagy of neural stem cells induced by heat stress via p38 MAPK/MK2/Hsp27−78 signaling pathway. *Biomed. Pharmacother.* **2019**, *114*, No. 108815.
(31) Fricker, M.; Tolkovsky, A. M.; Borutaite, V.; Coleman, M.; Brown, G. C. Neuronal Cell Death. *Physiol. Rev.* **2018**, *98*, 813−880.
(32) Turovskaya, M. V.; Gaidin, S. G.; Vedunova, M. V.; Babaev, A. A.; Turovsky, E. A. BDNF Overexpression Enhances the Preconditioning Effect of Brief Episodes of Hypoxia, Promoting Survival of GABAergic Neurons. *Neurosci. Bull.* **2020**, *36*, 733−760.
(33) Zhao, H.; Tang, J.; Chen, H.; Gu, W.; Geng, H.; Wang, L.; Wang, Y. 14,15-EET Reduced Brain Injury from Cerebral Ischemia and Reperfusion via Suppressing Neuronal Parthanatos. *Int. J. Mol. Sci.* **2021**, *22*, 9660.
(34) Epstein, Y.; Yanovich, R. Heatstroke. *N. Engl. J. Med.* **2019**, *380*, 2449−2459.
(35) Morrison, S. F. Central control of body temperature. *F1000Res* **2016**, *5*, 880.
(36) Morrison, S. F.; Nakamura, K. Central Mechanisms for Thermoregulation. *Annu. Rev. Physiol.* **2019**, *81*, 285−308.
(37) Bouchama, A.; Knochel, J. P. Heat stroke. *N. Engl. J. Med.* **2002**, *346*, 1978.
(38) Argaud, L.; Ferry, T.; Le, Q. H.; Marfisi, A.; Ciorba, D.; Achache, P.; Ducluzeau, R.; Robert, D. Short- and long-term outcomes of heatstroke following the 2003 heat wave in Lyon, France. *Arch. Intern. Med.* **2007**, *167*, 2177−2183.
(39) Sharma, H. S.; Hoopes, P. J. Hyperthermia induced pathophysiology of the central nervous system. *Int. J. Hyperthermia* **2003**, *19*, 325−354.
(40) Tan, C. L.; Knight, Z. A. Regulation of Body Temperature by the Nervous System. *Neuron* **2018**, *98*, 31−48.
(41) Zhang, Z. T.; Gu, X. L.; Zhao, X.; He, X.; Shi, H. W.; Zhang, K.; Zhang, Y. M.; Su, Y. N.; Zhu, J. B.; Li, Z. W.; Li, G. B. NLRP3 ablation enhances tolerance in heat stroke pathology by inhibiting IL-1β-mediated neuroinflammation. *J. Neuroinflammation* **2021**, *18*, 128.
(42) Yuan, R.; Wang, L.; Deng, Z. H.; Yang, M. M.; Zhao, Y.; Hu, J.; Zhang, Y.; Li, Y.; Liu, M.; Liu, S. F.; Zhou, F. H.; Zhu, H.; Kang, H. J. Experimental study on the protective mechanism of mesenchymal stem cells against central nervous system injury in heat stroke. *Curr. Stem Cell Res. Ther.* **2023**, *18*, 401.
(43) Zhang, Y.; Deng, Z.; Li, Y.; Yuan, R.; Yang, M.; Zhao, Y.; Wang, L.; Zhou, F.; Kang, H. Mesenchymal Stem Cells Provide Neuroprotection by Regulating Heat Stroke-Induced Brain Inflammation. *Front. Neurol.* **2020**, *11*, 372.
(44) Yi, J.; He, G.; Yang, J.; Luo, Z.; Yang, X.; Luo, X. Heat Acclimation Regulates the Autophagy-Lysosome Function to Protect Against Heat Stroke-Induced Brain Injury in Mice. *Cell. Physiol. Biochem.* **2017**, *41*, 101−114.
(45) Li, P.; Wang, G.; Zhang, X. L.; He, G. L.; Luo, X.; Yang, J.; Luo, Z.; Shen, T. T.; Yang, X. S. MicroRNA-155 Promotes Heat Stress-Induced Inflammation via Targeting Liver X Receptor α in Microglia. *Front. Cell. Neurosci.* **2019**, *13*, 12.
(46) Biedenkapp, J. C.; Leon, L. R. Increased cytokine and chemokine gene expression in the CNS of mice during heat stroke recovery. *Am. J. Physiol. Regul. Integr. Compar. Physiol.* **2013**, *305*, R978−R986.
(47) Lin, Y. F.; Liu, T. T.; Hu, C. H.; Chen, C. C.; Wang, J. Y. Expressions of chemokines and their receptors in the brain after heat stroke-induced cortical damage. *J. Neuroimmunol.* **2018**, *318*, 15−20.
(48) Chen, S. H.; Lin, M. T.; Chang, C. P. Ischemic and oxidative damage to the hypothalamus may be responsible for heat stroke. *Curr. Neuropharmacol.* **2013**, *11*, 129−140.

https://doi.org/10.1021/acsomega.3c03084
ACS Omega 2023, 8, 33392−33402

(49) Ko, W. C.; Lin, C. H.; Lee, J. J.; Chang, C. P.; Chao, C. M. Therapeutic Hypothermia Protects Against Heat Stroke-Induced Arterial Hypotension via Promoting Left Ventricular Performance in Rats. *Int. J. Med. Sci.* **2020**, *17*, 525−535. Research Paper. DOI: 10.7150/ijms.39745.
(50) Moniruzzaman, M.; Ghosal, I.; Das, D.; Chakraborty, S. B. Melatonin ameliorates H2O2-induced oxidative stress through modulation of Erk/Akt/NFkB pathway. *Biol. Res.* **2018**, *51*, 17.
(51) Hifumi, T.; Kondo, Y.; Shimizu, K.; Miyake, Y. Heat stroke. *J. Intens. Care* **2018**, *6*, 30.
(52) Wang, Y.; Dawson, V. L.; Dawson, T. M. Poly(ADP-ribose) signals to mitochondrial AIF: a key event in parthanatos. *Exp. Neurol.* **2009**, *218*, 193−202.
(53) Andrabi, S. A.; Kim, N. S.; Yu, S. W.; Wang, H.; Koh, D. W.; Sasaki, M.; Klaus, J. A.; Otsuka, T.; Zhang, Z.; Koehler, R. C.; Hurn, P. D.; Poirier, G. G.; Dawson, V. L.; Dawson, T. M. Poly(ADP-ribose) (PAR) polymer is a death signal. *Proc. Natl. Acad. Sci. U. S. A.* **2006**, *103*, 18308−18313.
(54) Zheng, L.; Wang, C.; Luo, T.; Lu, B.; Ma, H.; Zhou, Z.; Zhu, D.; Chi, G.; Ge, P.; Luo, Y. JNK Activation Contributes to Oxidative Stress-Induced Parthanatos in Glioma Cells via Increase of Intracellular ROS Production. *Mol. Neurobiol.* **2017**, *54*, 3492−3505.
(55) Chiu, L. Y.; Ho, F. M.; Shiah, S. G.; Chang, Y.; Lin, W. W. Oxidative stress initiates DNA damager MNNG-induced poly(ADP-ribose)polymerase-1-dependent parthanatos cell death. *Biochem. Pharmacol.* **2011**, *81*, 459−470.
(56) Leon, L. R.; Bouchama, A. Heat stroke. *Compr. Physiol.* **2015**, *5*, 611−647.
(57) Kravchenko, J.; Abernethy, A. P.; Fawzy, M.; Lyerly, H. K. Minimization of heatwave morbidity and mortality. *Am. J. Prevent. Med.* **2013**, *44*, 274−282.

https://doi.org/10.1021/acsomega.3c03084
ACS Omega 2023, 8, 33392−33402